SSRG International Journal of Electrical and Electronics Engineering
ISSN: 2348-8379/ https://doi.org/10.14445/23488379/IJEEE-V11I3P114

Volume 11 Issue 3, 178-186, March 2024

Original Article

Power Flow Analysis of On-Grid Photovoltaic Generation Using A Solid-State Transformer

Hanny H. Tumbelaka[1], Handry Khoswanto[2], Thiang[3], Stephanus A. Ananda[4]

[1,2,3]*Electrical Engineering Department, Petra Christian University, Indonesia.*
[4]*Informatic Department, Petra Christian University, Indonesia.*

[1]*Corresponding Author : thiang@petra.ac.id*

Received: 09 January 2024 Revised: 06 February 2024 Accepted: 07 March 2024 Published: 25 March 2024

Abstract *- This paper describes the power flow of a grid-connected PV system utilizing a Solid-State Transformer (SST). The SST system comprises a DC-AC converter, an isolated high-frequency step-up transformer, a bridge rectifier, and a Voltage Source Inverter (VSI). The DC-AC converter transforms the PV panel output voltage into a 5-kHz three-level square wave, where its pulse width regulates the PV load lines to generate power. The VSI delivers the PV power to the single-phase grid employing a grid current controller and a DC bus voltage controller. Computer simulation results verify the system's effectiveness in controlling the power flow from the PV panel through SST to the load and the grid while maintaining the grid current to be sinusoidal with a unity power factor, regardless of the presence of sunlight.*

Keywords *- Solid State Transformer, Grid-connected PV, Voltage Source Inverter (VSI), Three-level square wave, Photovoltaic.*

1. Introduction

Photovoltaic (PV) panels are commonly installed in both off-grid and on-grid configurations. In off-grid installation, electrical energy from the PV panel is only supplied to electrical loads and batteries as energy storage. Off-grid installation is suitable for remote areas. In some cases, the off-grid PV system works as a backup power source during power outages. In contrast, in on-grid installation, electrical energy that comes from the PV panel can be delivered to the grid and electrical loads.

The on-grid PV system does not need batteries or additional energy storage, making them cost-efficient and easy to maintain. The grid acts as a virtual storage system that allows sending or receiving electric power when needed. A Grid-Tie Inverter (GTI) is generally required for the on-grid PV system. The inverter converts a DC quantity into an AC quantity and can be synchronized to the grid.

The on-grid PV system has to be compatible with the grid. A potential issue with GTI arises because of the mismatch between PV panel output and grid voltage. The voltage difference can be adjusted with a transformer on the AC side or a boost converter on the DC side [1]. In addition, The PV panel usually needs galvanic isolation from the grid for safety and signal integrity reasons. The isolation can also be handled using a transformer. Typically, the existing transformer works at the standard grid frequency (50/60) Hz and has a large weight and size.

Nowadays, Solid-State Transformers (SST) have been developed and used for many applications, generally in distribution networks that connect the grid to the AC loads. SST is an AC-AC converter that combines a high-frequency transformer and power electronics converters [2-4]. The high-frequency transformer has a smaller weight and size than the conventional transformer (50/60 Hz). SST usually substitutes the conventional transformer [5, 6], where the medium voltage (20 kV) is stepped down to the low voltage (220/380 V) to meet customer equipment specifications. Several SST configurations are shown in Figure 1.

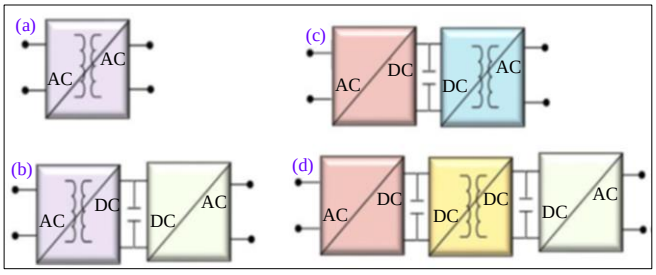

Fig. 1 Configurations of SST a) Single stage, b) and c) Two-stages, and d) Three stages [3].

Therefore, it is necessary to replace GTI with SST. SST will connect the grid to the DC source, the PV panel. SST also transmits the PV power to the grid. Several researches have been conducted on the application of SST for the on-grid PV system. In [7], an additional bidirectional buck-boost converter is used to get the PV power. Another system [8]

employs the SST topology featuring multilevel H-bridge for LV inverters and MV rectifiers and inverters. This paper presents an innovative SST configuration suitable for the on-grid PV system. Instead of adding circuits and controllers, an innovative approach involves simplifying the SST configuration for ease of operation and expansion.

Examining the power flow across the PV panel, load, and grid via SST is necessary to ensure this system works effectively. This analysis includes active and reactive power, comprising average and oscillating components. The analysis covers power flow at various loads and PV panel conditions, regardless of the presence of sunlight.

2. On-Grid PV Configuration

The chosen configuration for SST, as shown in Figure 1, is 1(d). It has three stages. Because the PV panel generates DC electricity, the AC-DC converter in the initial stage is removed. The PV panel is directly attached to the second stage, a DC-DC converter and this stage is named stage A. Stage A consists of three parts, i.e., a DC-AC converter, an isolated high-frequency transformer, and an AC-DC converter. Then, the stage A output is connected to a DC-AC converter, denoted as stage B, which is a Voltage Source Inverter (VSI). The VSI interfaces the stage A output to the power grid. Hence, a series circuit of stage A and stage B delivers electrical power from the PV panel to the power grid and load. Figure 2 illustrates the implementation of the on-grid PV system using SST.

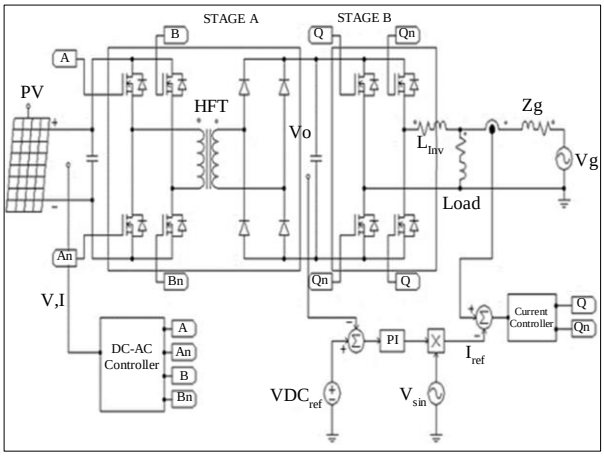

Fig. 2 Diagram of the grid-connected PV system

2.1. Solid State Transformer (SST)

The first component of stage A is the DC-AC converter, which generates the high-frequency AC voltage from the PV panel's DC output voltage since the transformer works at a high frequency. The converter consists of four transistors configured as an H-bridge. Switching of four transistors is controlled by using a microcontroller (DC-AC Controller). The switching operation can also drive the PV panel to generate maximum power. A simple concept algorithm used for this controller is shown in Figure 3. The microcontroller controls the switching time of the right and left legs of the H-bridge to produce square waves with a duty ratio of 50%. The square wave generated by each leg is phase-shifted by the displacement angle (α). As a result, the output voltage of the bridge will be a three-level AC square wave (Figure 4) with a pulse width of $180^o - \alpha$. The angle α determines the root mean square (*rms*) value of the square wave voltage as given in Equation 1. The PV panel output detects the *rms* value, which in turn dictates the PV panel's load lines (operating points). Figure 5 shows the load lines of the PV panel.

$$V_{sq-rms} = V_{dc}\sqrt{\frac{\pi-\alpha}{\pi}} \quad (1)$$

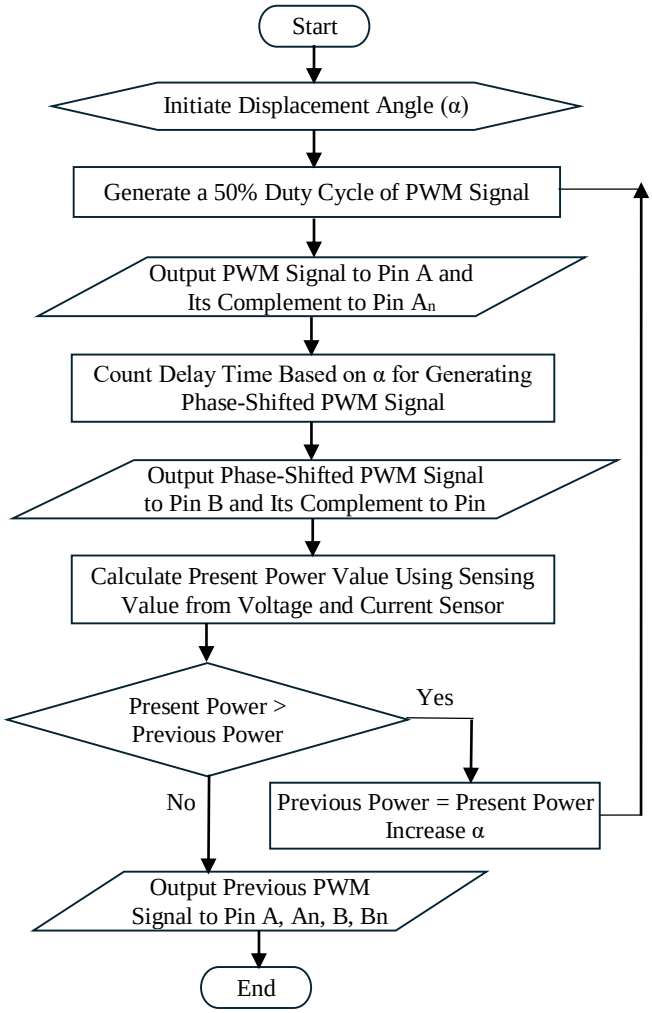

Fig. 3 Simple algorithm for controlling switching time

The isolated high-frequency transformer, as the second part of stage A, works at a frequency of 5 kHz. It is a two-winding step-up transformer, with the primary winding being supplied by the DC-AC converter and the secondary winding directed to the AC-DC converter. Its winding ratio is adjusted to match the PV panel output voltage level (≈ 35 V) to the VSI

input voltage level (DC Bus voltage ≈ 350 V). The transformer also provides galvanic isolation between the PV panel and the grid.

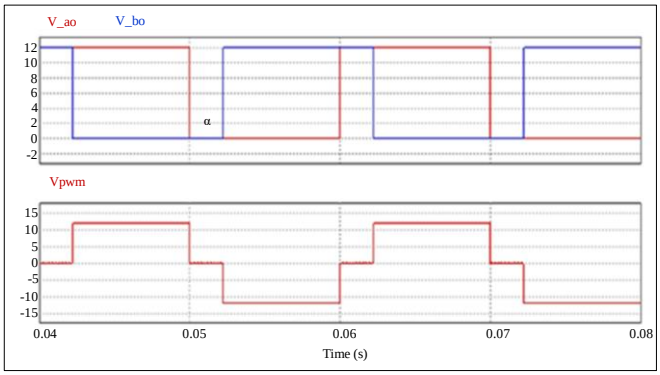

Fig. 4 Three-level square wave with a displacement angle α

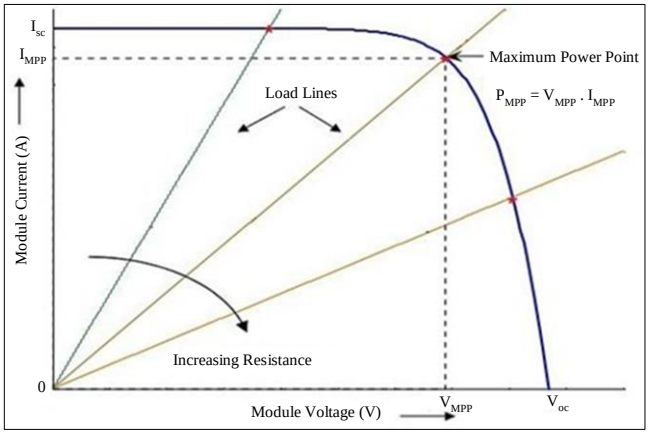

Fig. 5 Load lines of the PV panel [9]

The last part is an uncontrolled rectifier, which employs four diodes as an H-bridge. The rectifier converts a high-frequency AC voltage from the secondary side of the transformer to the DC bus voltage (V_o) of stage B. The diode bridge also prevents power reversal from the grid to the PV panel. The power flow becomes unidirectional from the PV panels to the grid and the load. A power capacitor is installed at the DC bus as an energy storage to reduce the voltage ripple.

2.2. The Grid-Connected Voltage Source Inverter

In stage B, the Voltage Source Inverter (VSI) uses four transistors as an H-bridge, with an inductor L_{inv} at the AC side, and connects the output of stage A to the single-phase power grid. Different from the previous DC-AC converter in stage A, in the VSI, the diagonally opposite transistors from the two legs are switched as switch pairs to produce a bipolar Pulse Width Modulation (PWM) square wave.

The VSI has a current controller and a voltage controller. The current controller has a current sensor on the grid side and senses the grid current. The output signal of the sensor is compared to the sinusoidal reference current (i_{ref}). The result is a high-frequency PWM signal to switch the transistors. By locating the current sensor on the grid side, the grid current controller can drive the grid current to be the same as the sinusoidal reference current (i_{ref}). This reference current is synchronized to the grid voltage and given by:

$$i_{ref}(t) = k \; v_{grid\text{-}1}(t) \quad (2)$$

Where $v_{grid\text{-}1}$ is the fundamental component of the grid voltage and k is the PI controller output. Consequently, the VSI automatically produces the current (i_{inv}) according to:

$$i_{grid}(t) = i_{inv}(t) + i_{load}(t) \quad (3)$$

The objective of the voltage controller is to maintain a constant DC bus voltage at its designated reference value. A voltage sensor is positioned at the DC bus to sense its voltage. The sensor output signal is compared to the DC bus reference voltage. The reference value should be greater than the amplitude of the grid voltage wave. Then, the error is controlled by a simple PI controller and produces a gain k. This gain k determines the amplitude of i_{ref} as written in Equation 2. This is an effective way of determining the required amplitude of grid active current since any active power mismatch among the grid, the load, and the VSI would result in the necessary corrections and regulate the DC bus voltage. The response speed of the voltage controller is considerably slower than that of the grid current controller, leading to the decoupling of the grid current controller and the voltage controller. Figure 6 reveals that the PI controller functions correctly. The DC bus voltage (V_o) is kept constant at 350 V.

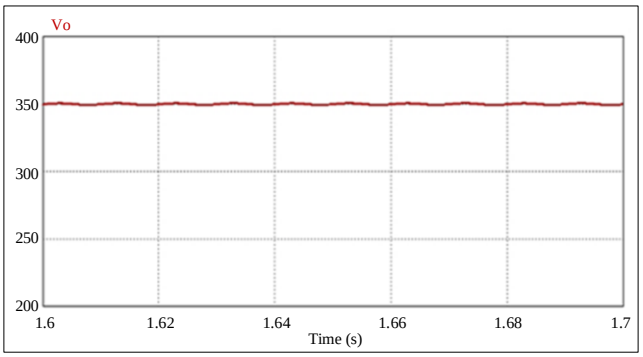

Fig. 6 DC bus voltage (V_o)

3. Power Flow

3.1. The PV Power

The power generated by the PV panel depends on the solar irradiance levels. Increased irradiance corresponds to higher PV output power. Moreover, at a specific irradiance level, the output power of the PV panel depends on its load lines, as illustrated in Figure 5.

As discussed earlier, changing the displacement angle (α) leads to changes in the *rms* value of the square wave voltage.

The rms value determines the load lines (operating points) of the PV panel. Hence, the PV panel output notices varying voltages, which affects its output power. The maximum power occurs when the voltage equals V_{MPP}.

3.2. The SST Power

For ideal converter conditions, the input power equals the output power. The converter transmits the received power to its output. In actual conditions, the significant losses in the converter occur in the form of switching losses, the amount of which depends on the switching frequency.

Similarly, the input power equals the output power for ideal transformer conditions. In actual conditions, there are core loss and copper loss. In SST, there is no energy conversion. The converter and transformer only transmit electric power from the PV panel. As discussed earlier, the power flow is unidirectional to the grid due to diodes in the rectifier.

3.3. The Grid Power

For a single-phase power grid, $v(t) = V \sin \omega t$, and $i(t) = I \sin (\omega t-\varphi)$. The instantaneous power will be [10, 11]:

$$p(t) = v(t)\, i(t) = VI\, cos\varphi\, (1 - cos2\omega t) - VI\, sin\varphi\, sin2\omega t \quad (4)$$

$$p(t) = P\, (1 - cos2\omega t) - Q\, sin2\omega t \quad (5)$$

The instantaneous power p(t) has two components. The first component oscillates twice the line frequency and has an average value of P = VI cosφ, denoted as active power. The second component also oscillates twice the line frequency with an amplitude equal to Q = VI sinφ, named reactive power. It has zero average value. The active power (P) can also be calculated as follows:

$$P = \frac{1}{T}\int_0^T v(t)\, i(t)\, dt \quad (6)$$

Due to the grid current controller, $i_{grid}\,(t) = I_{grid}\, sin\, \omega t$. The grid current is sinusoidal and has the same phase as the grid voltage, according to Equation 2. Since $\varphi = 0$, then Q = 0 and $p(t)$ in Equation 5 becomes:

$$p_{grid}(t) = P\, (1 - cos2\omega t) \quad (7)$$

The load current $i_{load}\,(t) = I_{load}\, sin\, (\omega t - \varphi)$. According to Equation 3, the output current of the VSI (i_{inv}) is given by:

$$i_{inv}(t) = I_{inv}\, (cos\varphi\, sin\omega t - sin\varphi\, cos\omega t) \quad (8)$$

It can be seen that the VSI current consists of two components which are active current and reactive current. The two currents are orthogonal and correspond to active power and reactive power, respectively.

The PV output power determines the amount of active power. Hence, the grid current control regulates the power flow of the grid, the VSI, and the load.

4. Simulation Results and Discussions

The circuit in Figure 2 is simulated using a PSIM simulator to prove the concept and to analyze the power flow- the circuit proceeds under steady-state conditions. The parameters used for the simulation are seen in Table 1.

Table 1. Circuit parameters

Parameters	Value
$V_{g\text{-}rms}$	220 V
Z_{grid}	0.02 Ω, 0.3 mH
L_{inv}	0.25 Ω, 1.51 mH
DC-Bus Capacitor	6600 μF
Transformer Ratio	1: 13
PV V_{mpp}	35.6 V
PV I_{mpp}	28.1A

4.1. The PV Output Power

The simulation focuses on the performance of the displacement angle control strategy to analyze the PV output power. The circuit in Figure 2 is tested under irradiance of 1000 W/m^2. Figure 7 shows the output voltage and current of the PV panel at maximum power. I_{pv} = 28.02 A, V_{pv} = 35.68 V, P_{pv} (max) = 999,8 W. The values of I_{pv} and V_{pv} are matched with the parameters specified in Table 1 for the PV panel.

To achieve the PV maximum power, the displacement angle (α) must be 29°. Figure 8 shows the output voltage of the DC-AC converter presenting a 5-kHz three-level square wave with a pulse width of 151°. V_{rms} = 32.74 V. This voltage is fed to the transformer's primary winding. The transformer's secondary voltage increases to 350 V (rms) due to its winding ratio, with the amplitude held equal to the DC bus voltage.

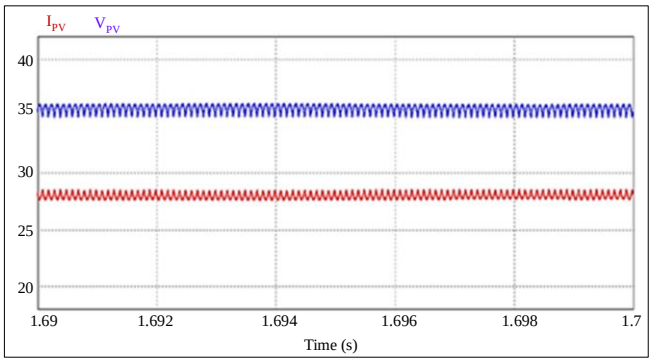

Fig. 7 PV output voltage and current for α = 29°

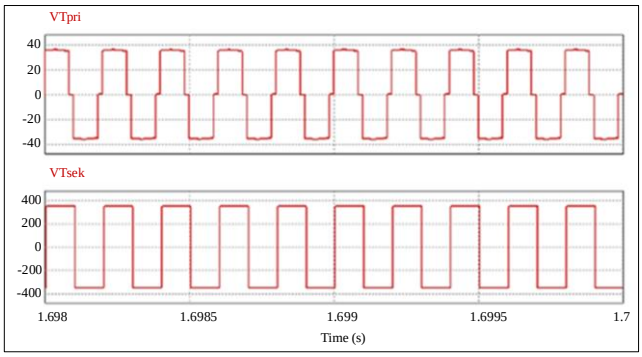

Fig. 8 Transformer primary (top) and secondary (bottom) voltages for α = 29°

If the displacement angle (α) is changed to 60°, the pulse width of the square wave becomes 120°. Then, the rms value of the output voltage of the DC-AC converter, which is the same as the transformer's primary voltage (Figure 10), changes to 31.14 V. As a result, the PV output voltage and current also change (Figure 9). I_{pv} = 25.31 A. V_{pv} = 37.92 V. P_{pv} = 959.4 W. This change indicates a decline in the PV output power compared to its maximum value.

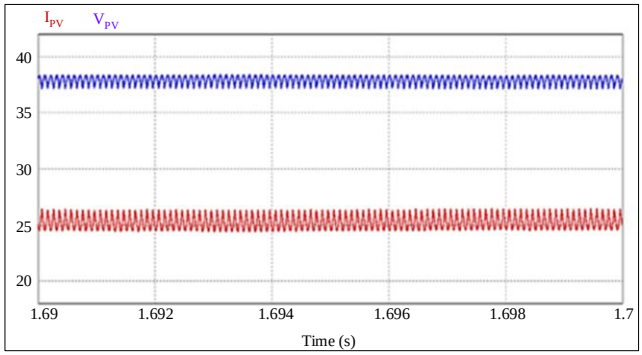

Fig. 9 PV output voltage and current for α = 60°

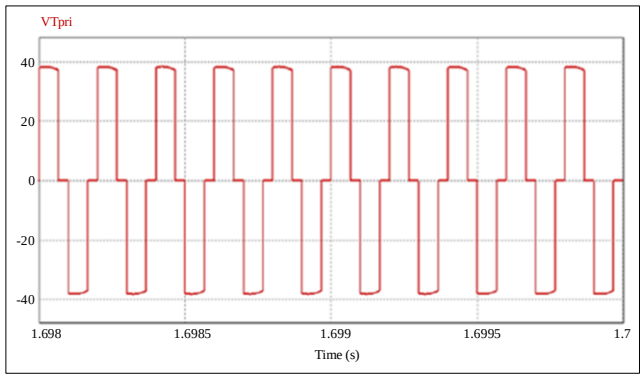

Fig. 10 Transformer primary voltage for α = 60°

For a similar case, Figure 11 displays the PV output voltage and current with an angle of 10°. The pulse width of the square wave equals 170°. I_{pv} = 28.41 A, V_{pv} = 35.12 V, P_{pv} = 997.76 W. It can be seen that the PV output power is also less than its maximum value. This is because the rms value of the output voltage of the DC-AC converter, which is the same as the transformer's primary voltage (Figure 12) for α = 10° becomes 34.29 V. The PV output power, the output voltage of the DC-AC converter, and the displacement angle (α) discussed before are summarized in Table 2.

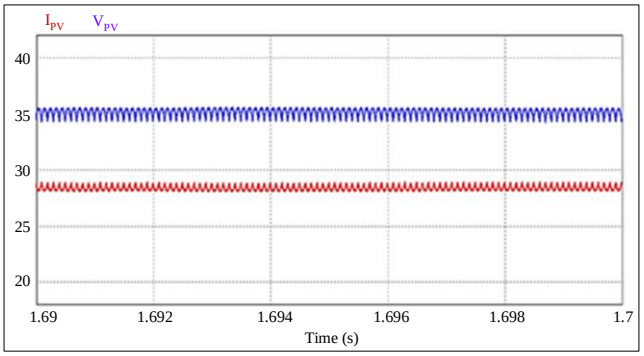

Fig. 11 PV output voltage and current for α = 10°

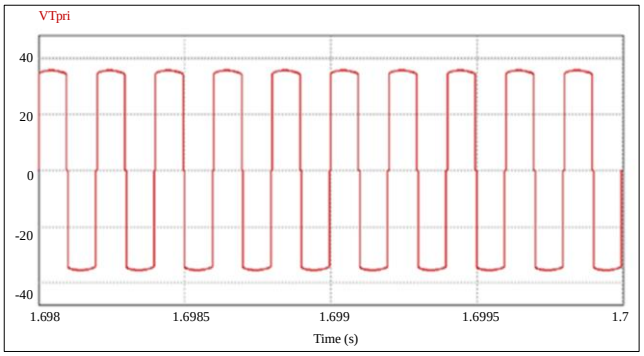

Fig. 12 Transformer primary voltage for α = 10°

Table 2. Displacement angle effects

α	V_{out} DC-AC converter (V_{rms})	I_{pv} (A)	V_{pv} (V)	P_{pv} (W)
10°	34.29	28.41	35.12	997.76
29°	32.74	28.02	35.68	999,81
60°	31.14	25.31	37.92	959.41

The controller will adjust the converter switching time according to the angle. The angle and pulse width of the square wave determine the rms value of the DC-AC converter output voltage. Increasing the angle leads to a decrease in the rms value of the voltage supplied to the high-frequency transformer and the PV output current but increases the PV output voltage.

However, PV output power will go up and down like a curve, with a maximum power point at α = 29°. Hence, the output power (load lines) of the PV panel corresponds to the displacement angle (α). Moreover, the transformer operates at variable voltage, which results in delivering variable power. The amount of power passing through stages A and B depends on the available power from the PV panel.

4.2. The VSI and The Grid Power

To evaluate the power flow among the grid, the VSI, and the linear (RL) load, the PV panel is operated at maximum power (P_{pv} = 999.81 W). The displacement angle (α) equals 29°. The VSI output power (P_{inv}) comes from the PV output power passing through stages A and B in series.

In the first case, the inverter (VSI) output power, in terms of active power, is greater than the load power. Figure 13 displays the grid voltage (top) and the currents of the grid, the VSI, and the load (bottom). Their rms values: I_{grid} = 1.79 A, I_{inv} = 4.62 A, I_{load} = 2.91 A.

Due to the grid current controller, Figure 13 also shows that the grid current waveform is forced to be the same as the sinusoidal reference current (i_{ref}). The grid current has the same zero crossing points as the grid voltage. Moreover, the VSI automatically produces a reactive current, as per Equation 8, to compensate for the reactive current of the load.

Figure 14 illustrates the grid power, the VSI power, and the load power. They oscillate at a frequency of 100 Hz. Based on Equations 5 and 6, their average values (active power): P_{grid} = –390.21 W, P_{inv} = 977.66 W, and P_{load} = 587.45 W. The grid power follows Equation 7 but flows in the reverse direction.

Since $P_{inv} > P_{load}$, the excess active power from the VSI is delivered to the grid. It is shown that the grid current is out of phase with the grid voltage, resulting in negative active power. The direction of the grid current, as well as the active power, is from the VSI to the grid.

Figure 15 shows the PI controller output signal (top) and i_{ref} (bottom). The sinusoidal reference current (i_{ref}) is obtained from Equation 2**.** The PI controller output (k) dictates its amplitude. The average value of k is negative (– 2.51). As a result, the phase difference between the grid voltage and the grid current is 180°.

In the second case, the inverter (VSI) output power, in terms of active power, is less than the load power. Figure 16 displays the grid voltage (top) and the currents of the grid, the VSI, and the load (bottom). Their rms values: I_{grid} = 3.79 A, I_{inv} = 4.95 A, I_{load} = 8.53 A. Figure 16 also shows that the grid current is sinusoidal with a unity power factor due to the grid current control. The correlation of the grid current, the VSI current, and the load current agrees with Equation 3. The direction of the grid current is from the grid to the load.

Figure 17 demonstrates the grid power, the VSI power, and the load power for the second case. Their frequency is 100 Hz. From Equations 5 and 6, their average values (active power): P_{grid} = 824.36 W, P_{inv} = 977.49 W, and P_{load} = 1801.85 W.

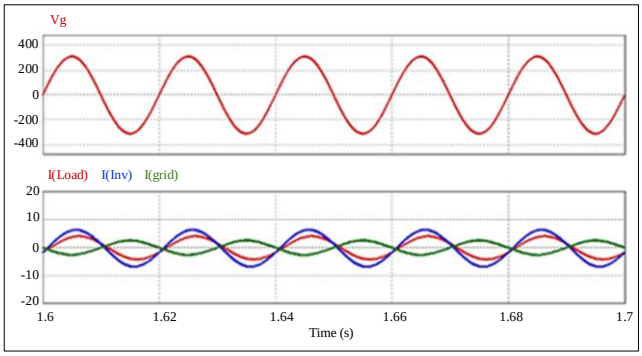

Fig. 13 The grid voltage (top) and the currents of the grid, the VSI, and the load (bottom) for $P_{inv} > P_{load}$

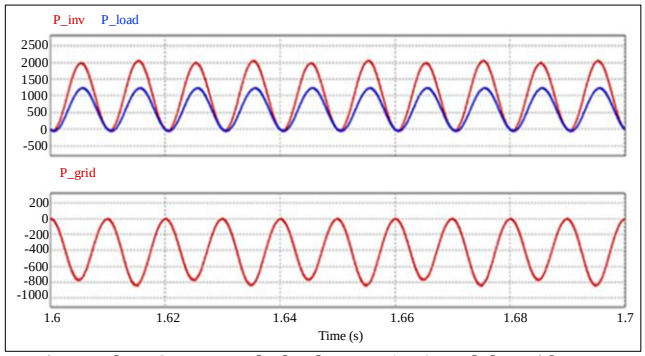

Fig. 14 The VSI power, the load power (top), and the grid power (bottom) for $P_{inv} > P_{load}$

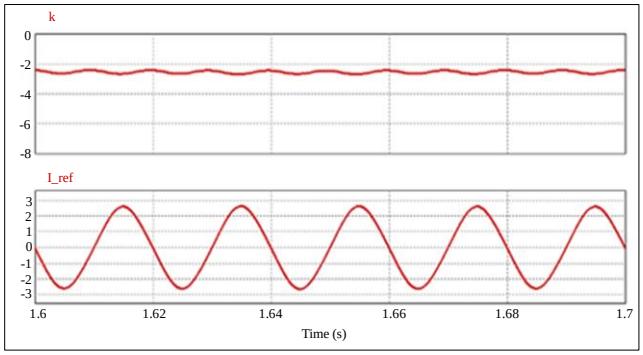

Fig. 15 The PI controller output signal (top) and i_{ref} (bottom) for $P_{inv} > P_{load}$

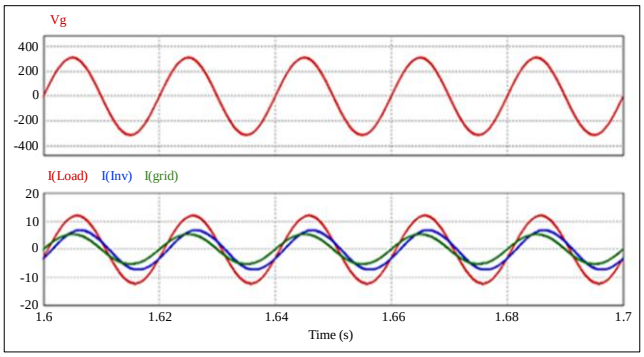

Fig. 16 The grid voltage (top) and the currents of the grid, the VSI, and the load (bottom) for $P_{inv} < P_{load}$

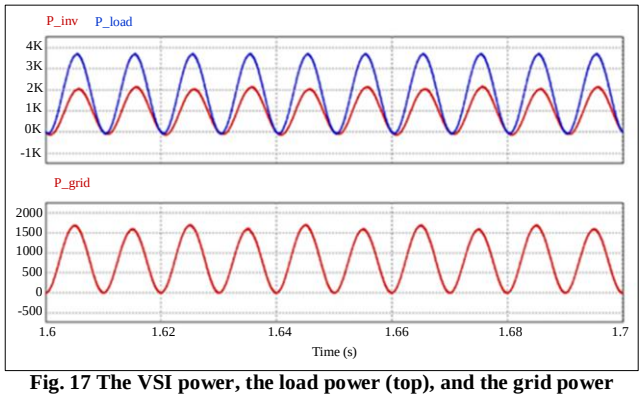

Fig. 17 The VSI power, the load power (top), and the grid power (bottom) for $P_{inv} < P_{load}$

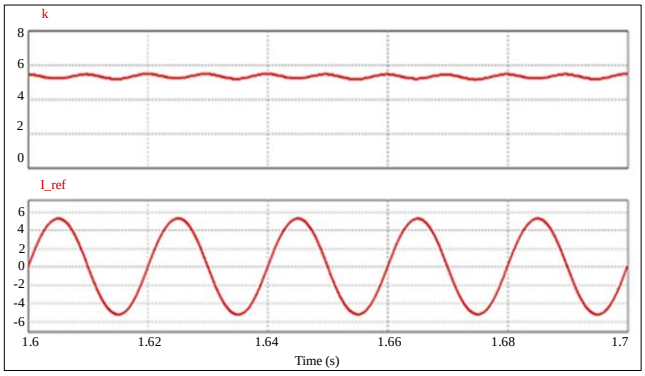

Fig. 18 The PI controller output signal (top) and i_{ref} (bottom) for $P_{inv} < P_{load}$

Since $P_{inv} < P_{load}$, the VSI output active power is insufficient for load power consumption. Then, the power deficit to supply the load is drawn from the grid. The grid power is positive and conforms with Equation 7. Figure 17 also shows that the VSI power comprises both active and reactive components.

The active power comes from the PV power and is supplied to the load. The reactive power corresponds to the presence of a reactive current component, as per Equation 8. The reactive power is used to compensate for the load reactive power.

Figure 18 shows the PI controller output signal (top) and i_{ref} (bottom). The average value of k has changed to 5.37. Hence, any mismatch in the system power flow will regulate the DC bus voltage and change the value of k, which will adjust the grid current amplitude. Because the value of k is positive, there is no phase difference between the grid voltage and the grid current.

The SST system can still function at night when the irradiance is very low. Figure 19 reveals the PV output voltage and current. There is no significant current flowing out from the PV panel. As a result, no electric power is delivered via the series of stage A and stage B to the load and the grid. The grid fully supplies the load of active power.

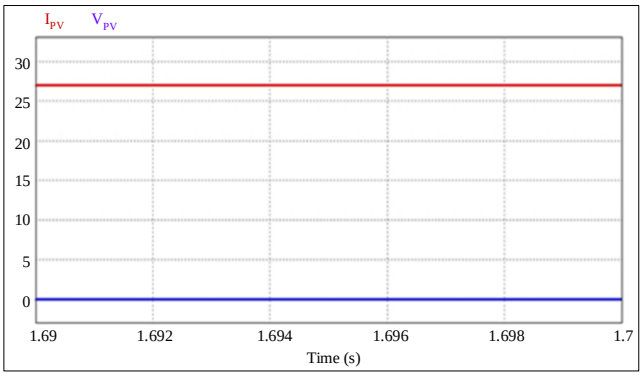

Fig. 19 PV output voltage and current for very low irradiance

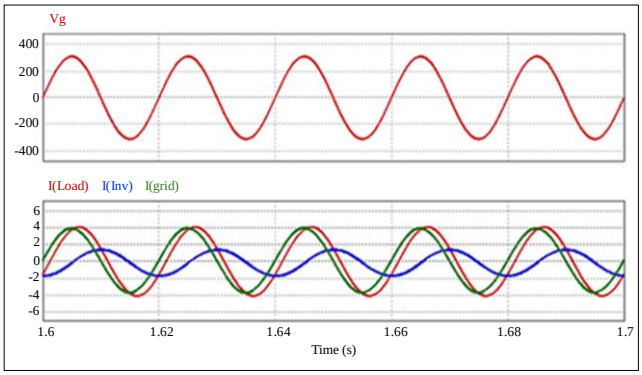

Fig. 20 The grid voltage (top) and the currents of the grid, the VSI, and the load (bottom) for very low irradiance

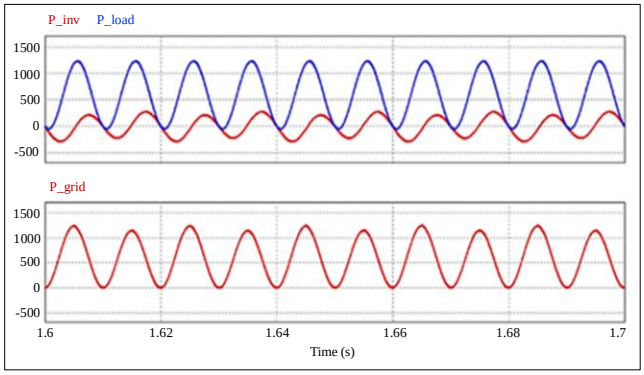

Fig. 21 The VSI power, the load power (top), and the grid power (bottom) for very low irradiance

However, the VSI still generates current. Figure 20 displays the grid voltage (top) and the currents of the grid, the VSI, and the load (bottom). Their rms values: Igrid = 2.72 A, Iinv = 1.12 A, Iload = 2.91 A. The grid current is similar to the load current.

Referring to Equation 8, when the active current is close to zero, then the VSI only generates the reactive current to compensate for the load reactive current. The phase angle between the grid voltage and the VSI current is around 90º. Figure 21 shows the grid power, the VSI power, and the load power. The average value of the VSI power is close to zero because there is no PV power.

Figure 22 shows the PI controller output signal (top) and i_{ref} (bottom). For very low irradiance, the average value of k has changed to 3.81. The value of k is positive, so there is no phase difference between the grid voltage and current.

The grid active power, The VSI output active power, and the load active power discussed above are summarized in Table 3. Table 3 also shows that there is no electric power from the grid flowing back to the VSI for both Pinv < Pload and Ppv ≈ 0. This is due to the diode rectifier in stage A, which prevents power reversal from the grid to the PV panel.

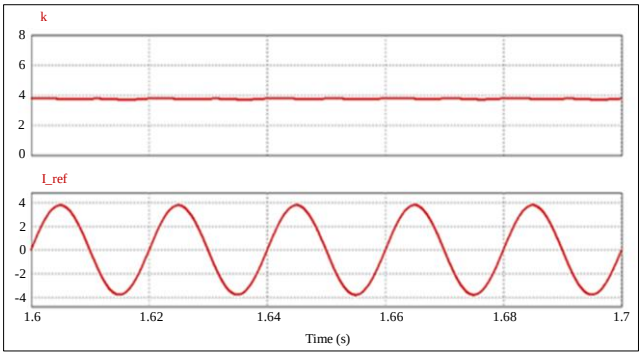

Fig. 22 The PI controller output signal (top) and i_{ref} (bottom) for very low irradiance

Table 3. Power flow

	P_{grid} (W)	P_{inv} (W)	P_{load} (W)
$P_{inv} > P_{load}$	–390.22	977.66	587.45
$P_{inv} < P_{load}$	824.37	977.49	1801.85
$P_{pv} \approx 0$	588.98	–1.26	587.72

5. Conclusion

This paper explains the power flow of a single-phase grid-connected PV system using a modified Solid-State Transformer (SST), which connects the PV panel to the grid. SST consists of a DC-DC converter (stage A) and a VSI (stage B). The DC-DC converter consists of a DC-AC converter, a two-winding isolated high-frequency transformer, and an uncontrolled rectifier.

To send solar energy to the load and grid, there are two control strategies. The first control strategy uses the pulse width of the three-level square wave to determine the PV load lines (operating points). The square wave is supplied to the primary winding of the high-frequency transformer.

The transformer operates at variable voltage, which results in delivering variable power. For the second control strategy, the VSI has a grid current controller and a DC bus voltage controller to regulate the flow of electrical power from the grid, the VSI, and the load. All of the control strategies are decoupled so they can work independently.

Computer simulation results using PSIM prove that the SST system works very well. The PV power is delivered to the load and the grid via a series circuit of stages A and B, while the grid current is sinusoidal and in phase with the grid voltage, regardless of the presence of sunlight or not.

Acknowledgments

The authors would like to thank The Ministry of Education, Culture, Research, and Technology, Indonesia, for the research grant and PT. Bambang Djaja, a Transformer Manufacturer, Indonesia for providing a high-frequency transformer.

References

[1] Doo-Yong Jung et al., "Interleaved Soft-Switching Boost Converter for Photovoltaic Power-Generation System," *IEEE Transactions on Power Electronics*, vol. 26, no. 4, pp. 1137-1145, 2011. [CrossRef] [Google Scholar] [Publisher Link]

[2] Hamed Shadfar, Mehrdad Ghorbani Pashakolaei, and Asghar Akbari Foroud, "Solid-State Transformers: An Overview of the Concept, Topology, and Its Applications in The Smart Grid," *International Transactions on Electrical Energy Systems*, vol. 31, no. 9, pp. 1-24, 2021. [CrossRef] [Google Scholar] [Publisher Link]

[3] Mahammad A. Hannan et al., "State of the Art of Solid-State Transformers: Advanced Topologies, Implementation Issues, Recent Progress, and Improvements," *IEEE Access*, vol. 8, pp. 19113-19132, 2020. [CrossRef] [Google Scholar] [Publisher Link]

[4] Scott D. Sudhoff, and W. Lafayette, "Solid State Transformer," *United States Patent*, Patent No. 5,943,229, 1999. [Online]. Available: https://patentimages.storage.googleapis.com/28/27/84/212fee1192da3b/US5943229.pdf

[5] Saleh A.M. Saleh et al., "Solid-State Transformers for Distribution Systems-Part I: Technology and Construction," *IEEE Transactions on Industry Applications*, vol. 55, no. 5, pp. 4524-4535, 2019. [CrossRef] [Google Scholar] [Publisher Link]

[6] Rogerio Luiz Da Silva et al., "Solid-State Transformer for Power Distribution Grid Based on a Hybrid Switched-Capacitor LLC-SRC Converter: Analysis, Design, and Experimentation," *IEEE Access*, vol. 8, pp. 141182-141207, 2020. [CrossRef] [Google Scholar] [Publisher Link]

[7] Kunati Madhu, and V. Sunil Kumar Reddy, "Grid-Connected PV-Wind-Battery Based Multi-Input Transformer Coupled Bidirectional DC-DC Converter with Multilevel Inverter Fed AC Load," *International Journal of Scientific Engineering and Technology Research*, vol. 6, no. 32, pp. 6588-6593, 2017. [Google Scholar] [Publisher Link]

[8] G. Brando, A. Dannier, and R. Rizzo, "Power Electronic Transformer Application to Grid-Connected Photovoltaic Systems," *International Conference on Clean Electrical Power*, Capri, Italy, pp. 685-690, 2009. [CrossRef] [Google Scholar] [Publisher Link]

[9] S.M. Ferdous et.al., "Design and Simulation of an Open Voltage Algorithm based Maximum Power Point Tracker for Battery Charging PV System," *7th International Conference on Electrical & Computer Engineering (ICECE)*, Dhaka, Bangladesh, pp. 908-911, 2012. [CrossRef] [Google Scholar] [Publisher Link]

[10] E.H. Watanabe et al., "New Concepts of Instantaneous Active and Reactive Powers in Electrical Systems in Generic Loads," *IEEE Transactions on Power Delivery*, vol. 8, no. 2, pp. 697-703, 1993. [CrossRef] [Google Scholar] [Publisher Link]

[11] F.Z. Peng, L.M. Tolbert, and Zhaoming Qian, "Definitions and Compensation of Non-Active Current in Power Systems," *33rd Annual IEEE Power Electronics Specialists Conference*, Australia, vol. 4, pp. 1779-1784, 2002. [CrossRef] [Google Scholar] [Publisher Link]